Application Note

Super-Resolution in Label-Free Photomodulated Reflectivity

Zurich Instruments

Applications: Thermoreflectance, NPMR, super-resolution microscopy
Products: UHFLI, UHF-AWG, UHF-MF

Release date: March 2017

Introduction

This Application Note details a far-field, label-free super resolution (SR) microscopy approach which relies on inducing a spatial distribution of physical properties, such as temperature or carrier concentration, by an ultrashort laser pulse within the photo-excited diffraction limited spot. By monitoring the nonlinear response of any property of the sample, which depends on this spatial distribution, for example the temperature, label-free spatial information with higher resolution as given by the diffraction limit may be extracted.

PSF and SR definitions in the photo-modulated image

The theoretical background behind the nonlinear photo-modulated reflectance (NPMR), which is an example of our approach to label-free super resolution microscopy, is discussed in details in Refs. [1, 2]. Though NPMR originates from numerous physical effects, we will focus our discussion on thermal excitation and the probing of thermoreflectance (TR). In TR one uses the changes of reflectance upon heating to measure thermal properties of materials or to map heating using linear models. Measuring nonlinear components of TR in response to photo-excitation allows the significant reduction of the effective point spread function (PSF), leading to an enhanced resolution.
The image resolution in case of linear TR is determined by the pump and probe intensity profiles, the pump-probe time delay, and the scanned object. In our analysis we consider a temperature profile identical to the laser Gaussian intensity distribution with standard deviation σ_{pump}, which is valid for short pump-probe delays of about 0–3 ps. The probe beam has a Gaussian shape with standard deviation σ_{probe}.
Consequently, the linear TR image P(x,y) comprises the product of the pump and probe images, convolved with the object function O(x,y):

$$\begin{aligned} P(x,y) &= (PSF_{pump} \cdot PSF_{probe}) \otimes O(x,y) \\ &= PSF_{TR} \otimes O(x,y) \\ &= I_{pump} e^{-\frac{r^2}{2\sigma_{pump}}} I_{probe} e^{-\frac{r^2}{2\sigma_{probe}}} (t=0) \otimes O(x,y). \end{aligned}$$

We can extract the effective point spread function in the linear TR, PSF_{TR}, by deconvolution of the image with the object, resulting in a Gaussian function with a standard deviation of

$$\sigma_{TR} = \sqrt{\frac{\sigma_{pump}^2 \sigma_{probe}^2}{\sigma_{pump}^2 + \sigma_{probe}^2}}.$$

For a pump beam with half the wavelength of the probe, the resolution enhancement over an electrically heated sample with the same diffraction-limited

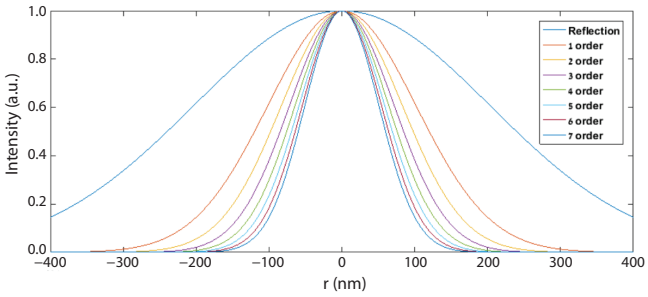

Figure 1. Simulated profiles of the effective PSF on the on the lateral (r) axis calculated from the PSF and the n-th order of the pump intensity distribution. The blue curve represents a probe reflection scan, while the other curves correspond to the n-th order of TR.

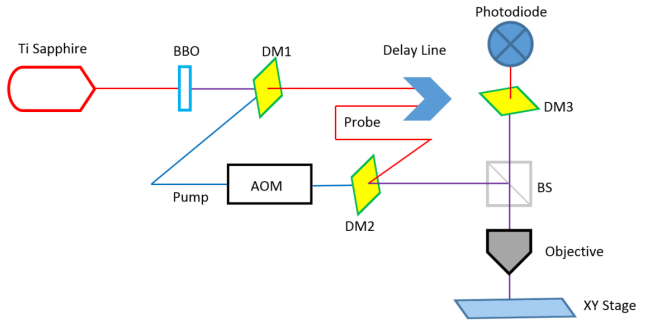

Figure 2. Optical setup comprising dichroic mirrors (DM), an acousto-optic modulator (AOM), a beam splitter (BS), and a photodiode.

probe beam is $\sqrt{5}$. In the case of identical wavelengths for pump and probe beams this improvement is only $\sqrt{2}$. Incorporating pump-induced non-linearities improves the resolution beyond the linear case.
For a given delay between pump and probe, the relative change in reflectivity as a function of temperature T, can be represented as a Taylor series:

$$\frac{\Delta R}{R}(\alpha, T) = a_1(\alpha)T + a_2(\alpha)T^2 + a_3(\alpha)T^3 + \cdots$$

where α is a material dependent parameter. If the pump excitation is a pure sine wave with modulation frequency ω, the temperature is also a harmonic function, $T(\alpha) = Ib_0(\alpha)e^{i\omega t}$, where the parameter b_0 depends on the material and relates the incoming intensity I to the temperature. The time-dempendent thermoreflectance $\Delta R/R$ is then given by

$$\frac{\Delta R}{R} \approx a_1 I e^{i\omega t} + a_2 I^2 e^{i2\omega t} + a_3 I^3 e^{i3\omega t} + \cdots$$

where we omitted the dependencies on α for the sake of readability. By detecting the modulation at different harmonics of ω, the non-linear response is measured. The nonlinear intensity profile measured at 2ω, 3ω,... is a Gaussian to the power of n=2, 3,...., which is narrower than the first-order Gaussian as shown in Figure 1. We thus expect to achieve a higher resolution.
In order to measure the nonlinear response of the physical system, it is mandatory to excite the system with pure harmonic light intensity without distortions. In the following we describe how we use an acousto-optic modulator (AOM), which inherently produces distorted light modulation, together with the UHFLI Lock-in Amplifier and the UHF-AWG Arbitrary Waveform Generator to produce a pure sinusodial excitation.

Experimental Setup

The optical setup is illustrated in Figure 2. An 800 nm beam (probe) with 100 fs pulse duration at the source is frequency-doubled to 400 nm (pump). The beams are separated by a dichroic mirror. A variable delay line is used to tune the timing of the probe relative to the probe beam and a subsequent dichroic filter combines the two beams into a reflection microscope.
The pump beam at 400 nm is modulated at 54 kHz using an AOM together with the UHF-AWG as shown in Figure 4. To satisfy the drive voltage requirements of the AOM RF driver, we make use of the possibility to generate an AWG signal on one of the Auxiliary Outputs which provide a larger signal amplitude than the Signal Output of the UHFLI. The AWG output signal for the AOM is tailored as to produce a pure sinusoidal optical excitation. The probe reflectance is measured at different harmonics of the reference frequency using a photodiode and a UHFLI lock-in amplifier. In order to phase-lock the drive signal with the lock-in detection, we generate a sinusoidal signal on Auxiliary Output 1 and feed it back into Ref / Trigger Input 1 to be used as a lock-in reference signal.
The code block in Fig. 3 shows the LabOne AWG Sequencer program used for this experiment. The customized waveform aux_ch2 used to generate the modulation signal is loaded from an external file, whereas the sinusoidal waveform aux_ch1 for the reference signal is created directly in the program. The two waveforms aux_ch1 and aux_ch2 are then played back to back in an infinite loop. The frequency of the generated signals is then defined by the AWG sampling rate when using the Auxiliary Outputs, 14.0625 MHz, divided by the number of samples in the waveform, 256.

```
// Auxiliary Output 1 signal:
// Generate sine waveform as phase reference
// for the UHF lock-in amplifier (feed to Ref/
    Trigger)
const samples = 256;
const phase = 0; const periods = 1;
wave aux_ch1 = sine(samples, phase, periods);
// Auxiliary Output 2 signal:
// read waveform from the file modulation.csv
wave aux_ch2 = 'modulation';

// Play the signals with infinite repetition
while (true)
{
  playAuxWave(aux_ch1, aux_ch2, AWG_RATE_14MHZ);
}
```

Figure 3. LabOne AWG Sequencer program used for the experiment.

Measurement Result and Analysis

The technique of measuring higher harmonics of the TR relies on having a purely sinusoidal pump intensity modulation. Since the AOM has a nonlinear transfer function, its input signal should be distorted in a controlled manner in order to generate a pure harmonic output. Thanks to the multiple demodulators of the UHFLI, we are able to measure the fundamental and higher harmonics of the modulated light intensity. These data are fed to an iterative algorithm that we developed, which updates the AWG signal applied to the AOM in order to reduce the nonlinear components of

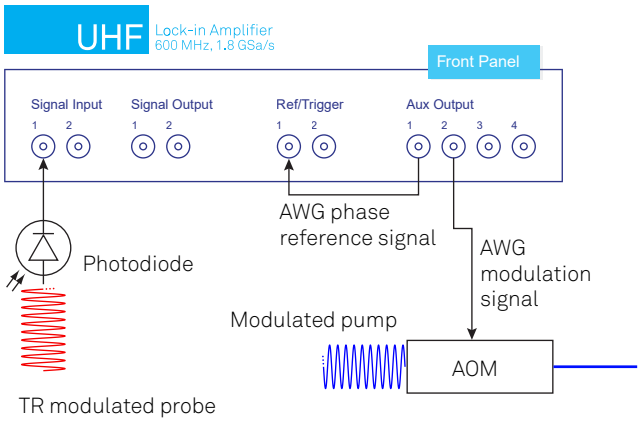

Figure 4. Electrical setup used to generate the pump beam modulation and to measure the photodiode signal. The AWG output on Auxiliary Output 1 is connected to the AOM driver. The photodiode signal is measured with the UHFLI. The Ref/Trigger connectors are used to phase-lock the UHF-AWG with the lock-in amplifier.

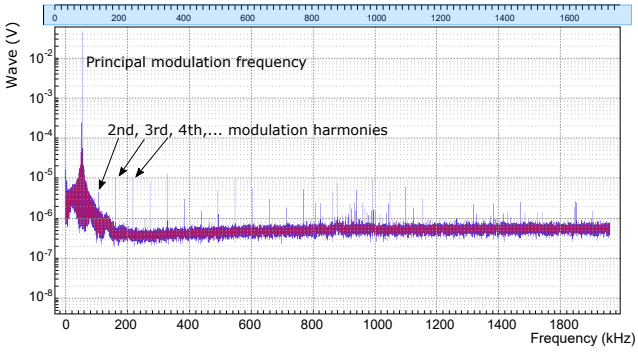

Figure 5. Pump signal's Fourier transform measured with the Oscillsoscope of LabOne user interface. The plot shows a prominent peak at the principal modulation frequency 54 kHz, while the 2nd, 3rd, 4th,... harmonics are about 80 dB below the amplitude of the main peak.

the pump laser modulation. The details of this method will be published in a future article. As an alternative to the AWG, the UHF-MF Multi-frequency option provides the functionality to superpose up to 8 harmonics with individual amplitudes and phases on the Signal Output to fine-tune the AOM drive signal.

The Fourier transform of the pump signal is shown in Figure 5, showing a prominent main peak at 54 kHz while the peaks at higher harmonics are at least 4 orders of magnitude lower, thus verifying the requirement for pure sinusoidal excitation.

The SR scan of gold double lines on ITO nanostructures is shown in Figure 6 (c-e). Fitting a two-Gaussian model to the signal of 2nd harmony from the 4th pair of gold double lines (160 nm gap), yields a full width at half maximum (FWHM) of 227.5±6.1 nm and 209.2±5.6 nm for first and second peak, respectively, and a gap distance of 178±2 nm. A similar fit for the 3nd harmony signal yields a FWHM of 142.9±16 nm and 151.1±16.5 nm for the first and second peak, respectively, and a gap distance of 180±2 nm.

The calculated gap matches closely with the measured gap size of 161 nm from the HR-SEM image in Figure

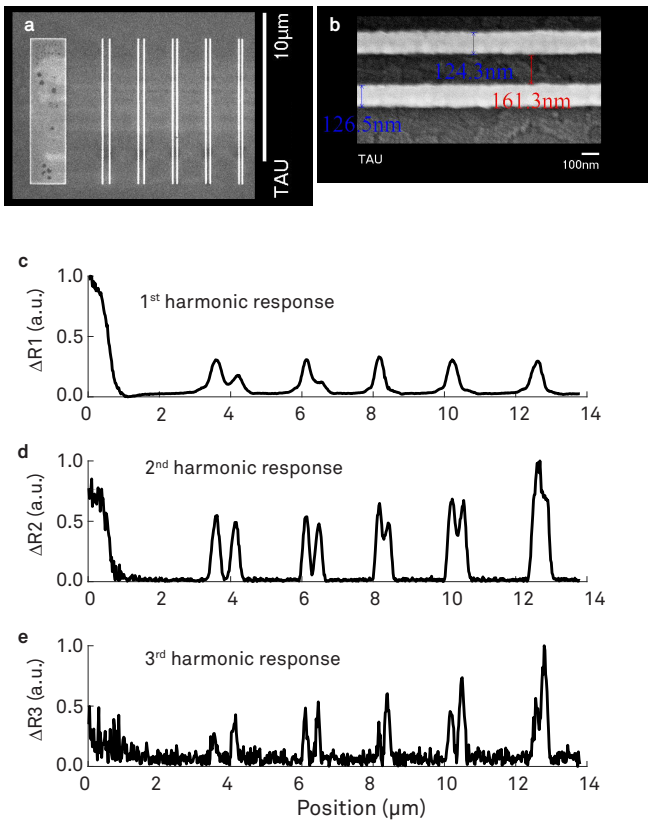

Figure 6. Super-resolution line imaging of gold on sapphire nanostructures. The sample consists of gold double lines, 125 nm wide, with decreasing gaps of 370, 270, 160, 160, and 120 nm, respectively. (**a**) High-resolution scanning electron microscope (HR-SEM) image of the sample. (**b**) HR-SEM zoom on one of the 160 nm gap double lines. (**c-e**) Line scan with a 0.95 NA objective using the 1st (**c**), 2nd (**d**), and 3rd (**e**) harmonic of the modulation.

6 (b). Moreover, the narrowing of the FWHM by a factor of 1.5 corresponds well with the expected theoretical narrowing of the PSF by a factor of 1.34.

The multiple demodulators of the UHFLI enable us to measure the thermoreflectance response at multiple harmonics simultaneously which ensures that all signals are acquired under the exact same experimental conditions. In addition, this option immensely simplifies the experimental setup, as the alternative would be to use multiple lock-in amplifiers or to extend the data acquisition time in order measure the harmonics sequentially.

Combining the drive and measurement in a single instrument helps reducing the risk for electrical cross talk and ground loops between different devices. This is particularly important in measurements of the nonlinear response signal, which is small and can easily drown in electronic noise.

Conclusion

In this application note we described the procedure of super-resolution optical microscopy in a label-free sample using photomodulated reflectivity measured with the UHFLI. The multi-purpose digital nature of

the UHFLI greatly helps simplifying this experimental method by providing an all-in-one hub for the required A/D signal generation and detection. The ability for multi-harmonics demodulation and FFT readout is crucial for the generation and verification of a pure harmonic modulation. The simultaneous measurement of several harmonics saves measurement time and eliminates the need for multiple lock-in amplifiers.
The resolution of this method can be enhanced further by recording higher-order nonlinearities. The practical limit of attainable resolution is governed by lower power and signal-to-noise ratio in high harmonic response. Increasing the laser power to achieve higher nonlinearity is bracketed by the sample damage threshold.

Acknowledgements

Zurich Instruments would like to thank Dror Hershkovitz, Omer Tzang, Haim Suchowski, and Ori Cheshnovsky from Tel Aviv University for contributing this application note.

References

[1] Omer Tzang and Ori Cheshnovsky. Far-field super-resolution microscopy based on the nonlinear response of photothermal excitation. Proc. SPIE 9361, Ultrafast Phenomena and Nanophotonics XIX, page 93610T, March 14, 2015.

[2] Omer Tzang, Alexander Pevzner, Robert E. Marvel, Richard F. Haglund, and Ori Cheshnovsky. Super-resolution in label-free photomodulated reflectivity. Nano Letters, 15(2):1362–1367, 2015.

Zurich Instruments
Technoparkstrasse 1
CH-8005 Zurich
Switzerland
www.zhinst.com
info@zhinst.com
+41 44 515 04 10